



UNIVERSITY OF LEEDS

This is a repository copy of *Some aspects of modeling NO<sub>x</sub> formation arising from the combustion of 100% wood in a pulverized fuel furnace.*

White Rose Research Online URL for this paper:  
<http://eprints.whiterose.ac.uk/89255/>

Version: Accepted Version

---

**Article:**

Darvell, LI, Ma, L, Jones, JM et al. (2 more authors) (2014) Some aspects of modeling NO<sub>x</sub> formation arising from the combustion of 100% wood in a pulverized fuel furnace. *Combustion Science and Technology*, 186 (4-5). 672 - 683. ISSN 0010-2202

<https://doi.org/10.1080/00102202.2014.883834>

---

**Reuse**

Unless indicated otherwise, fulltext items are protected by copyright with all rights reserved. The copyright exception in section 29 of the Copyright, Designs and Patents Act 1988 allows the making of a single copy solely for the purpose of non-commercial research or private study within the limits of fair dealing. The publisher or other rights-holder may allow further reproduction and re-use of this version - refer to the White Rose Research Online record for this item. Where records identify the publisher as the copyright holder, users can verify any specific terms of use on the publisher's website.

**Takedown**

If you consider content in White Rose Research Online to be in breach of UK law, please notify us by emailing [eprints@whiterose.ac.uk](mailto:eprints@whiterose.ac.uk) including the URL of the record and the reason for the withdrawal request.



[eprints@whiterose.ac.uk](mailto:eprints@whiterose.ac.uk)  
<https://eprints.whiterose.ac.uk/>

# SOME ASPECTS OF MODELLING NO<sub>x</sub> FORMATION ARISING FROM THE COMBUSTION OF 100% WOOD IN A PULVERIZED FUEL FURNACE

L.I. Darvell\*, L. Ma\*\*, J.M. Jones\*, M. Pourkashanian\*\*, A. Williams\*\*.

[fueaw@leeds.ac.uk](mailto:fueaw@leeds.ac.uk)

\*Energy Research Institute, Leeds University, Leeds LS2 9JT

\*\*Energy Technology and Innovation Institute, Leeds University, Leeds LS2 9JT

## Abstract

Over the last decade there has been considerable interest in modeling the co-combustion of coal and biomass with biomass levels up to about 20 wt%. Because of increasing environmental concern about the emission of CO<sub>2</sub>, there has recently been a move in some countries to use near 100% of biomass. This action has raised a number of issues, and one of these is the control of the NO<sub>x</sub> formed. The factors relating to the formation and in-furnace control of NO<sub>x</sub> from wood are considered in this article, and it is concluded that the main route is via HCN.

Keywords: Modeling; NO<sub>x</sub> formation; Pulverized wood combustion

## Introduction

The use of biomass as a fuel in existing coal-fired power systems has been used as a means of reducing environmental emissions. Up to the present time, the co-firing of coal with up to typically 20% biomass has been widely implemented in large-scale plants (Backreedy et al., 2005; Gera et al., 2002; Mathur et al., 2002; Ma et al. 2009; Sami et al., 2001). However, there is a need to increase the amount of biomass to more than 90% due to environmental pressures. With these larger amounts of biomass, there can be problems with ash deposition and unburned carbon in ash, since conventional coal mills are unable to pulverize biomass into small enough particle sizes (Backreedy et al., 2005; Gera et al., 2002). As far as acid gas emissions are concerned, SO<sub>x</sub> is decreased because of the lower fuel sulfur content. But in the case of NO<sub>x</sub> emission, although the amount of fuel-N is small on a mass basis (relative to coal), on a thermal basis it may still be just as significant. Since burning biomass with low sulfur content can result in the dispensation of the need for SO<sub>x</sub> removal from the flue gases, the question arises as to whether this can be the case for NO<sub>x</sub> also.

NO can be formed by the thermal mechanism, by prompt-NO or from fuel-NO in an analogous way to coal (Skreiberg et al. 1997, Ma et al. 2007, Stubenberger et al. 2008). In bituminous coal combustion, the heterocyclic N-compounds form mainly HCN, but in biomass, fuel-N can exist both as heterocyclic compounds and as amino acid groups in proteins. Hence, NO can be formed from the HCN intermediate produced from the heterocyclic compounds, while the protein nitrogen can be converted into both HCN and NH<sub>3</sub> intermediates and ultimately NO together with some HNCO (Darvell et al., 2012; Hansen and Glarborg, 2010; Hansson et al., 2003a, 2003b; Ren et al., 2011; Stubenberger et al. 2008). The protein nitrogen content of wood has been estimated to be in the range of 70–90 wt.% of the total nitrogen, and therefore a combination of both the HCN and NH<sub>3</sub> routes has to be

considered. There also seems to be some limited evidence that the amount of HCN given off increases with temperature (Hansen and Glarborg, 2010; Hansson et al., 2003b).

With biomass, generally other factors come into play: first, the difficulty in accurately measuring the fuel-N content, and second, the variability both in total N content in biomass samples and types. For example, with straw, natural senescence leads to a lower N content due to reduced protein-N, although leaving a relatively higher proportion of heterocyclic aromatic compounds. It has been suggested (Darvell et al., 2011; Di Nola et al., 2010; Ohtsukaan et al., 1997) that the amount of ammonia given off is also a function of the potassium present, that is, low potassium-containing wood evolves mainly HCN and a little NH<sub>3</sub>, while high potassium-containing fuels give mainly NH<sub>3</sub>. This may be partially due to the catalytic effect of the alkali species in biomass, which may promote the formation of both N<sub>2</sub> and NH<sub>3</sub> from HCN and tar-N. Many of these nitrogen compounds can form potassium derivatives, but details of a possible reaction route are not yet understood.

This article looks at some of the issues involved and in particular in the light of a previous investigation by Ma et al. (2007) that is concerned with the CFD modeling of NO formation from wood combustion. This work was coupled with experimental tests on firing pure biomass, which had been carried out at the 1 MW pulverized fuel combustion test facility (CTF) situated at the E.ON New Build and Technology Centre at Ratcliffe, UK. The CTF consists of a single burner in a combustion chamber with an over-fire air facility. The combustor is a three-staged, wall-fired, low-NO<sub>x</sub> swirl burner of generic design widely used in large-scale power utilities (Mitsui-Babcock Mark III). The furnace is fully refractory-lined and water-cooled. The CTF was designed to replicate the time–temperature history of a coal particle entering a full-scale, wall-fired power station furnace.

### CFD Modelling Studies

The fuel that was employed is a soft wood commonly used in power generation with the properties listed in Table 1. The milled fuel as received is in a wide range of particle shapes, typically with a fraction of flat chip and cylindrical shapes and also with some small spherical particles. The aspect ratio of the particles received is usually very high, typically in the magnitude of 10. The fuel feed rate was 0.0517 kg/s and the particle sizes used were 90–1500 μm (average 320 μm). The total flow air in was 0.285 kg/s, 19% of which used as over firing air, and the splits were as follows for primary/secondary/tertiary/over-fire air: 1/1.3/1.4/0.9.

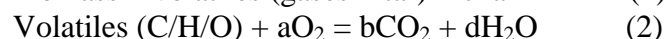
Table 1 here

The CFD model used has been previously described, including details of the computational mesh and boundary conditions used by Ma et al. (2007) and is shown in Figure 1. The commercial software ANSYS Fluent was used as before, together with many of the default sub-programs. The effect of the turbulence on the reaction has been modeled with the eddy dissipation turbulence–chemistry interaction model and the RNG-k–ε turbulence model.

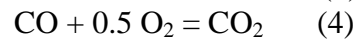
The P1 radiation model was used for the furnace heat transfer calculations.

Fig 1 here

The combustion model consists of a devolatilization step followed by combustion of the volatiles and char as set out below. Each combustion step is associated with an NO- forming reaction. The reaction steps are as follows:



The reaction rate was calculated based on the eddy-dissipation model, which depends on the mass fraction of the reactants/products and the reaction stoichiometric coefficients. The char is oxidized further to CO:



A single rate temperature dependent devolatilization model expressed in an Arrhenius form was employed. The data for the kinetic rate of the volatile release is calculated using the network program, FG-Biomass (Advanced Fuel Research, AFR Inc.). The values obtained for the pre-exponential factor and the activation energy for wood are  $A = 6 \times 10^{13} \text{ 1/s}$  and  $E = 2.5 \times 10^8 \text{ J/kg mol}$ . The values used in this model may be subject to debate, since there is a considerable diversity in the values of kinetic data in the literature.

In high temperature combustion of pulverized wood at high heating rates, we assume that pyrolysis products do not form tar and give the equivalent amount of CO and H<sub>2</sub>. There is no experimental evidence for tar formation under these conditions, except perhaps in very rich mixtures. The density was taken to be 550 kg/m<sup>3</sup>, and the specific heat was taken to 1670 J/kg K.

The composition of the volatiles that has been used in the simulation was estimated in two ways. First, it was based on the data in Table 1, from the proximate and ultimate analyses of the fuel. During volatile combustion, the organic part of the volatiles is oxidized to form CO<sub>2</sub> and water in the gas stream. For the CFD modeling of the oxidation of the volatile species, it was taken to be an organic compound with a formula of C/H/O, so a global one-step reaction mechanism being employed.

The N in the fuel is partitioned between the volatiles and the char on the basis of the carbon distribution. It is a reasonable estimate and is approximately consistent with the experimental values given in Table 1. In the case of the volatiles, the NO was calculated on the basis of the assumption of either HCN or NH<sub>3</sub> being formed from the fuel N and the De Soete global equations employed for either one case or the other. In our previous investigation (Ma et al., 2007), we concluded that the ratio of the HCN route to the NH<sub>3</sub> route was 3:1.

Alternatively, the pyrolysis products can be calculated more exactly using FG- Biomass. The results are given in Table 2 and are based on the previous assumption, that the tar is all converted to CO and H<sub>2</sub>.

Table 2 here

It can be seen that there is some considerable difference between the assumptions of single component (volatiles) combustion and the combustion of the actual pyrolysis products shown in Table 2. This difference is more important in flame stability considerations rather than in the calculation of NO<sub>x</sub> formation.

The CFD modeling of biomass char combustion is more complicated than for coal char. This is because it is influenced not only by the composition of the biomass, especially the oxygen content in the char and the presence of catalytic metals, but also by the shape and size of the particles, since biomass particles mainly keep their original irregular shape during devolatilization. Often the process leads to a partially activated char with a high surface area, which results in a higher reactivity of biomass in the later stages of combustion (Williams et al., 2012).

Therefore, here we model char combustion using Smith's intrinsic model and increased the reaction rate by a factor of four in order to represent the high burning rate of the biomass char particles (Williams et al., 2012). NO formation was assumed to take place directly from the char-nitrogen, with the rate being proportional to the rate of carbon consumption.

A number of CFD simulations have been performed on biomass combustion in the E.ON Combustion Test Facility. Figure 2a shows the typical trajectories of the biomass particles predicted in the furnace, colored by the particle residence time, when the majority of the particles have not yet fully penetrated the furnace. The typical particle residence time calculated is about 5 s, while some of the particles may stay over 10 s. Particles lose mass rapidly just after the front of the burner and this is where the main drying, devolatilization, and fuel-N reactions proceed. When they have reached the vertical chamber of the furnace, most of the particles have become much lighter, but a significant number of particles are observed to fall to the bottom of the furnace due to gravity. These particles consist of both large sized particles and the particles that have not completely devolatilized. The prediction is consistent with the experimental observations.

Figure 2b shows the oxygen concentration in the furnace, and the effect of the over- fire air is clearly seen. There is no experimental data available to show if this is a true representation of the real situation in the furnace. But these results show that the influence cannot be highly effective and that the flow of gases leaving the furnace is not uniform.

Fig 2 here

Computations were also made of the temperature profile shown previously by Ma et al. (2007), but here detail is shown of the NO<sub>x</sub> formation routes. Both the HCN and the NH<sub>3</sub> routes were considered for NO<sub>x</sub> formation using the equations developed by De Soete (1975). The computed results for NO formation via the HCN route are shown in Figure 3a, and the concentration of the HCN intermediate is given in Figure 3b. Figures 4a and 4b similarly show NO formed via the NH<sub>3</sub> route as well as the concentration of the NH<sub>3</sub> intermediate. It is clear that the NH<sub>3</sub> reacts near to the burner, while in contrast (Figure 3b), some of the HCN survives through the body of the furnace and is only finally destroyed when it meets the over-fire air.

At the exit of the furnace, a NO concentration of 280 ppmv has been predicted using the NH<sub>3</sub> mechanism only. When using the HCN mechanism alone, the calculated NO was 90 ppmv. However, using a combination of the two, on a 1:3 basis (this means 1 NO from NH<sub>3</sub> and 3 NO from HCN), yields a predicted concentration of 137 ppmv NO, which is similar to the 140 ppmv found experimentally. This is consistent with the values of HCN and NH<sub>3</sub> calculated using FG-Biomass and with a protein content of 70–90% of the total nitrogen content.

The De Soete equations give the rate of the oxidation of HCN to NO and reduction to N<sub>2</sub> respectively:

$$R_{\text{oxid}} = 1 \times 10^{10} X_{\text{HCN}} [X_{\text{O}_2}]^n \exp\{-280.4/RT\} \text{ s}^{-1}$$

$$R_{\text{RED}} = 3 \times 10^{12} X_{\text{HCN}} X_{\text{NO}} \exp\{-251.2/RT\}$$

and for ammonia

$$R_{\text{oxid}} = 4 \times 10^6 X_{\text{NH}_3} [X_{\text{O}_2}]^n \exp\{-133.9/RT\}$$

$$R_{\text{RED}} = 1.8 \times 10^8 X_{\text{NH}_3} X_{\text{NO}} \exp\{-113.0/RT\}$$

where  $R_i$  are the reaction rates,  $X_i$  the mol fraction, and  $n$  is the reaction order, which is zero for  $X_{O_2}$  greater than 3 mol% oxygen. Clearly the relative rate of formation of NO from the two routes is very temperature-dependent and is subject to experimental error as recognized in the original work by De Soete. These correlations were obtained in flame studies and are strictly only applicable for a limited temperature range, which is above that found in furnace flames, as well as for a narrow range of specific concentrations of fuel-N compounds and the NO formed. However, there is considerable evidence that these correlations are sufficiently accurate for CFD modeling in coal flames (Álvarez et al., 2012; Cao et al., 2010), probably because the rate of formation of NO is controlled by the rate of release of the nitrogen-containing intermediates from the coal rather than by gas phase chemistry.

Fig 3 here

From Figure 3, a number of features can be identified:

1. The computed NO formation rates based on the De Soete equations are consistent with the experimental observations. There is evidence (see below) that the  $NH_3$  route is chemically faster, although the reverse is the case with the De Soete equations alone. The controlling step is however the rate of pyrolysis of the biomass and release rate of the fuel-N compounds since the rate of the oxidation/reduction of both HCN and the  $NH_3$  is extremely rapid as shown later.
2. It appears that the effect of OFA may not be properly computed, probably because the chemistry in that region is too simplified.
3. The effect of particle size can be important; any large particles will carry unburned fuel and hence fuel or char-N through the reducing staged regions; on combustion in the main body of the furnace will directly produce NO. The geometric position of the over-fire air, the % OFA and the distribution of the injected air are important in this respect. If it is too closely coupled, it may not be able to deal with large particles as yet unburned.

### **Global Modelling NO<sub>x</sub> Formation: Zonal Approach**

The zones involved are effectively the same as those described above for the CFD model, but the different zones are treated as separate entities so as to be able to include more detailed chemistry. The zones considered are combustion under (i) staged conditions where the NO<sub>x</sub> produced results from the homogeneous reactions of HCN and  $NH_3$ ; this includes consideration of mainly the primary zone but also the effects of the addition of the secondary and tertiary air; (ii) the formation of NO<sub>x</sub> from the N-containing char in the main body of the furnace; and (iii) the influence of the over-fire air. The computer code CHEMKIN-Pro (Reaction Design, USA) was used for the calculations.

The staged combustion zone involves the fuel-rich combustion with the primary air, and the injection of the secondary and then tertiary air. Here the total air is 0.285 Kg/s, 19% of which is used as over-firing air, and the primary/secondary/tertiary split was 1:1.2:1.3. This arrangement can be modeled using a homogeneous kinetic mechanism and is very dependent on the assumptions of mixing and the stoichiometric ratio assumed in the primary flame zone. In a previous article, we calculated the influence of staging for coal devolatilization products (Chaiklangmuang et al., 2002), and a similar scenario holds for biomass devolatilization products. In the case of the coal products, which are similar to the wood pyrolysis products because of the large amount of HCN, the amount of conversion to NO is small once the equivalence ratio is rich of stoichiometric, the calculated amount being less than 5% as shown in Figure 5, but the actual computed extent depends on the choice of the kinetic scheme chosen. However, in addition to the NO, there is a considerable amount of HCN, which still

remains at the end of the time allocated for combustion in the primary zone. The assumptions of residence time and temperature are not the major controlling factors, since the composition of the products is mainly determined by the equivalence ratio.

Similar calculations have been made using biomass pyrolysis products calculated by FG-Biomass and in which the tar is considered to be decomposed to CO and H<sub>2</sub>. Typical computed results are shown in Figures 6 and 7. Figure 6 shows that as previously shown (Hansen and Glarborg, 2010), the ammonia burns out first and the HCN more slowly. This is paralleled by the burn-out of CO shown in Figure 7 showing that the HCN and CO are not completely burned in the primary zone of a staged burner; this will be even more likely if there are large particles that are not completely devolatilized in the primary zone. This is expected for the CO, because the role of the secondary and tertiary air and the OFA is to complete the combustion of these species. But if the HCN is incompletely reacted, the reaction sequence in the region between the staged burner and the OFA involves complex chemistry including HCN, CO, and the intermediate species such as HNCO. Combustion of the char and char-nitrogen can likewise form HNCO.

These calculations show, as is expected, that at the end of the primary zone, there is a significant amount of unburned HCN remaining. The temperature chosen of 1000 K represents the temperature at which the pyrolysis products are released; the products formed are not significantly temperature-dependent. The role of the secondary and tertiary air is important, so the HCN and CO are combusted without forming significant amounts of NO. It can be shown that if the secondary air is added and well stirred with the products from the primary zone, then the amount of NO is considerably increased. Therefore the strategy for the design of the primary and secondary zones is that the primary zone has to be as rich as possible to allow stable burning, and the secondary zone has to be effectively overall sub-stoichiometric to permit the reduction of the remaining HCN without forming significant amounts of NO. The effect of the tertiary air is then to slightly cool and dilute the combustion products.

Figure 8 shows the influence of the added secondary air stream in a coflow situation (calculated by CHEMKIN-Pro) on the NO formation. The temperature in the mixing zone is important because it is increased by the combustion of the incoming combustible products from the primary zone. Clearly the stoichiometry of this zone is important, and the way this is done in practice will determine the success of the staging arrangement in the burner. In the case here, it is simply undertaken by mixing in a coflowing system, but the effects are clear. The HCN is rapidly oxidized forming some additional NO, which is then diluted and cooled slightly by the tertiary air stream.

The amount of char produced at high heating rates is about 10 wt% of the original fuel, and the particle sizes are dependent on the initial particle size distribution of the milled biomass. These particles are responsible for about 20% of the thermal release into the furnace, and the N contained in them is responsible for a considerable amount of the NO formed. If the larger biomass particles are not combusted in the reducing regions of the staged burner, then the N in them is carried through to the upper regions of the furnace producing NO there.

During the char burn-out, NO<sub>x</sub> is also produced from the thermal-NO<sub>x</sub> reactions. This is very dependent on the oxygen content and on the temperature of the boiler, which is a function of the accuracy of the computation or measurement of the furnace temperature. Since both of these are difficult to undertake with any precision, there will be uncertainties, especially since it is dependent on the extent and nature of the slag on the furnace walls. With 3% excess

oxygen and a 3s residence time, a furnace with a uniform temperature of 1575 °C produces 150 ppm thermal NO<sub>x</sub>, at 1550 °C it produces 82 ppm, and at 1500 °C it produces 34 ppm. The influence of over-fire air is shown in Figure 2 for the CFD calculation, but it is effectively a NO dilution effect. It does however result in some burn-out of the CO, since the exhaust CO concentration is in accord with the experimental value.

## Conclusions

The calculation of NO using fairly conventional CFD methods has been examined in the light of more detailed reaction modeling. While CFD methods give good agreement with the levels of NO observed, many aspects are not well described, especially the immediate influence of the tertiary air and the reactions in the main body of the furnace, which are additional to thermal NO<sub>x</sub> reactions.

The interaction with the over-fire air has not been investigated in detail here, but it is clear that the optimization of this stage is extremely important and could be a major NO<sub>x</sub> reduction strategy in certain circumstances.

## Acknowledgements

We wish to thank Dr. D. J. Waldron and Dr. M. Wojtowicz for helpful discussions.

## References

- Álvarez, L., Gharebagh, M., Jones, J.M., Pourkashanian, M., and Williams, A., Riaza J, et al. 2012. Numerical investigation of NO emissions from an entrained flow reactor under oxy-coal conditions. *Fuel Process. Technol.*, 93, 53–64.
- Backreedy, R.I., Fletcher, L.M., Jones, J.M., Ma, L., Pourkashanian, M., and Williams, A. 2005. Co-firing pulverised coal and biomass: A modelling approach. *Proc. Combust. Inst.*, 30, 2955–2964.
- Cao, H., Sun, S., Liu, Y., and Wall, T.F. 2010. Computational fluid dynamics modeling of NO<sub>x</sub> reduction mechanism in oxy-fuel combustion. *Energy Fuels*, 24, 131–135.
- Chaiklangmuang, S., Jones, J.M., Pourkashanian, M., and Williams, A. 2002. Conversion of volatile-nitrogen and char-nitrogen to NO during combustion. *Fuel*, 81, 2363–2369.
- CHEMKIN-Pro. Reaction Design, San Diego, CA. <http://www.reactiondesign.com>.
- Darvell, L.I., Jones, J.M., Ma, L., Pourkashanian, M., and Williams, A. 2011. Modelling NO<sub>x</sub> formation in pulverised coal and biomass co-fired boiler units. In *Proceedings of the Bioten Conference on Biomass, Bioenergy and Biofuels*, September, Birmingham, UK, 2010; A. V. Bridgwater (Ed.), CPL Press, Newbury, UK, pp. 854–858.
- Darvell, L.I., Brindley, C., Baxter, X.C, Jones, J.M., and Williams A. 2012. Nitrogen in biomass char and its fate during combustion—a model compound approach. *Energy Fuels*, 26, 6482–6491.
- De Soete, G.G. 1975. Overall reaction rates of NO and N<sub>2</sub> formation from fuel nitrogen. *Proc. Combust. Inst.*, 15, 1093–1102.
- Di Nola, G., de Jong, W., and Spliethoff, H. 2010. TG-FTIR characterization of coal and biomass single fuels and blends under slow heating rate conditions: Partitioning of the fuel-bound nitrogen. *Fuel Process. Technol.*, 91, 103–115.
- FG-Biomass. Advanced Fuel Research, AFR Inc. <http://www.afrinc.com>.
- Gera, D., Mathur, M.P., Freeman, M.C., and Robinson A. 2002. Effect of large aspect ratio of biomass particles on carbon burnout in a utility boiler. *Energy Fuels*, 16, 1523–1532.
- Hansen, S., and Glarborg, P. 2010. A simplified model for volatile-N oxidation. *Energy Fuels*, 24, 2883–2890.

- Hansson, K.-M., Amand, L.-K., Habermann, A., and Winter, F. 2003. Pyrolysis of poly-L-leucine under combustion-like conditions. *Fuel*, 82, 653–660.
- Hansson, K.-M., Samuelsson, J., Amand, L.-E., and Tullin, C. 2003. The temperature's influence on the selectivity between HNCO and HCN from pyrolysis of 2,5-diketopiperazine and 2-pyridone. *Fuel*, 82, 2163–2172.
- Ma, L., Gharebaghi, M., Porter R., Pourkashanian, M., Jones, J.M., and Williams, A. 2009. Modelling methods for co-fired fuel furnaces. *Fuel*, 88, 2448–2454.
- Ma, L., Jones, J.M., Pourkashanian, M., and Williams, A. 2007. Modelling the combustion of pulverized biomass in an industrial combustion test furnace. *Fuel*, 86, 1959–1965.
- Ohtsukaan, Y., Zhihenga, W., and Furimsky, E. 1997. Effect of alkali and alkaline earth metals on nitrogen release during temperature programmed pyrolysis of coal. *Fuel*, 76, 1361–1367.
- Ren, Q., Zhao, C., Chen, X., Duan, L., Li Y., and Ma, C. 2011. NO<sub>x</sub> and N<sub>2</sub>O precursors (NH<sub>3</sub> and HCN) from biomass pyrolysis: Co-pyrolysis of amino acids and cellulose, hemicellulose and lignin. *Proc. Combust. Inst.*, 33, 1715–1722.
- Sami, M., Annamalai, K., and Wooldridge, M. 2001. Co-firing of coal and biomass fuel blends. *Prog. Energy Combust. Sci.*, 27, 171–214.
- Skreiberg, O., Glarborg, P., Jensen, A., and Dam-Johansen, K. 1997. Kinetic NO<sub>x</sub> modeling and experimental results from single wood particle combustion. *Fuel*, 76, 671–682.
- Stubenberger, G., Scharler, R., Zahirovic, S., and Obernberger I. 2008. Experimental investigation of nitrogen species release from different solid biomass fuels as a basis for release models. *Fuel*, 87, 793–806.
- Williams, A., Jones, J.M., Ma, L., and Pourkashanian, M. 2012. Pollutants from the combustion of biomass. *Prog. Energy Combust. Sci.*, 38, 113–117.

## Tables

**Table 1.** Chemical and thermo physical properties of the fuel (wt% ar.)

Ultimate analysis (wt.% ar)			
C	H	N	K
47.80	5.90	0.17	0.26
Proximate analysis (wt.% ar)			
Moisture	Volatile matter	Fixed carbon	Ash
10.1	69.4	18	2.5

**Table 2.** Composition of the pyrolysis products from wood.

Species	Concentration mol %
CO	0.347
CO <sub>2</sub>	0.022
H <sub>2</sub> O	0.195
H <sub>2</sub>	0.391
CH <sub>4</sub>	0.037
NH <sub>3</sub>	0.00108
HCN	0.00738

## Figures

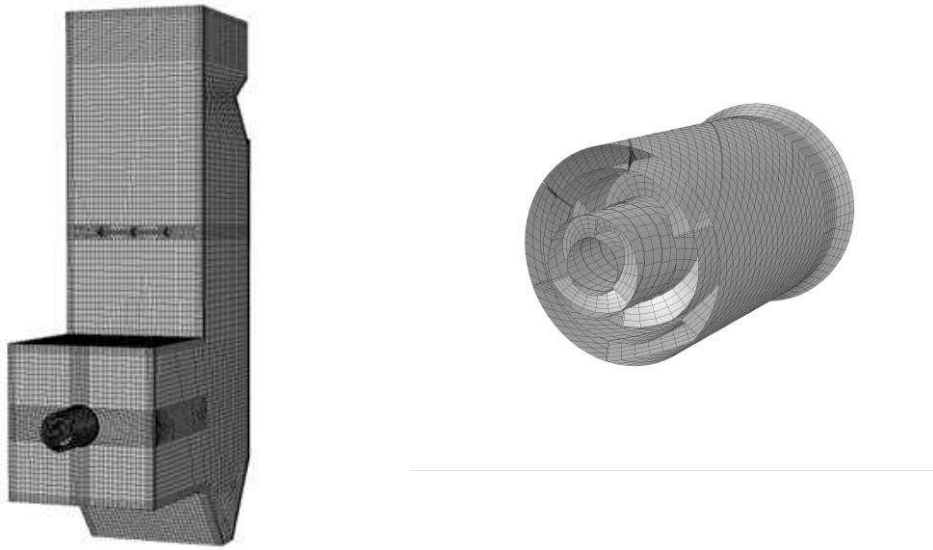


**Figure 1.** The E.ON Combustion Test Facility showing details of the burner.

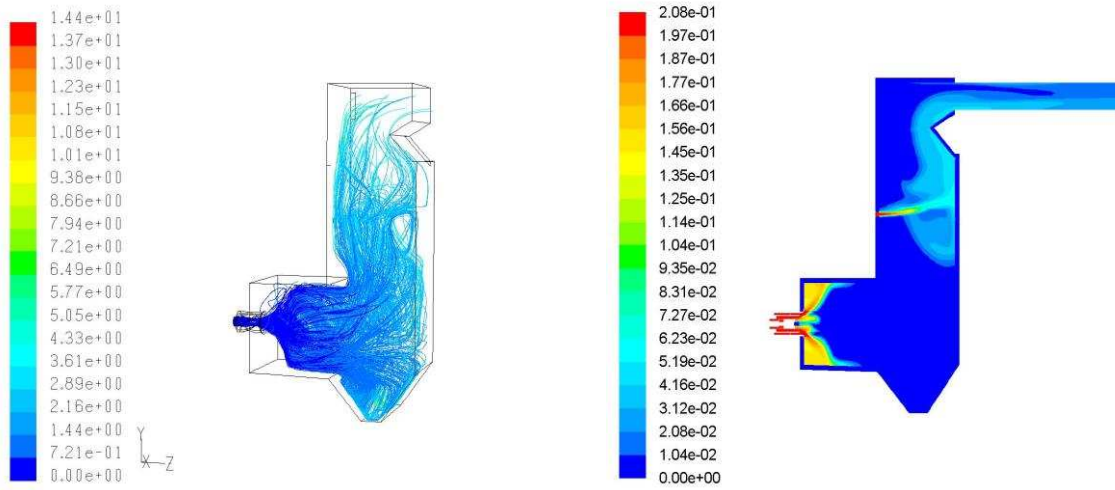


**Figure 2** (a) Particle residence times. (b) Computed O<sub>2</sub> concentration profiles (mol fraction).

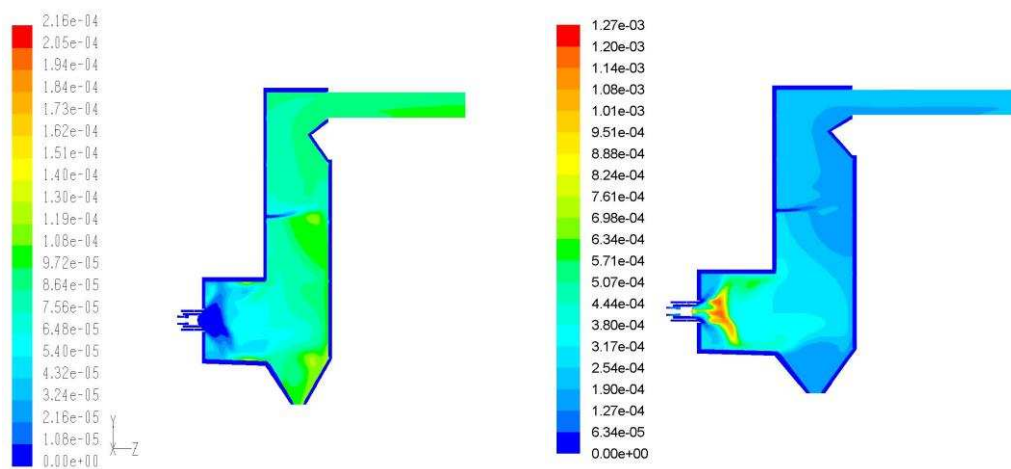


**Figure 3** (a) Computed NO<sub>x</sub> profile assuming HCN intermediate route only and using the De Soete equation. (b) HCN concentration (mol fraction).

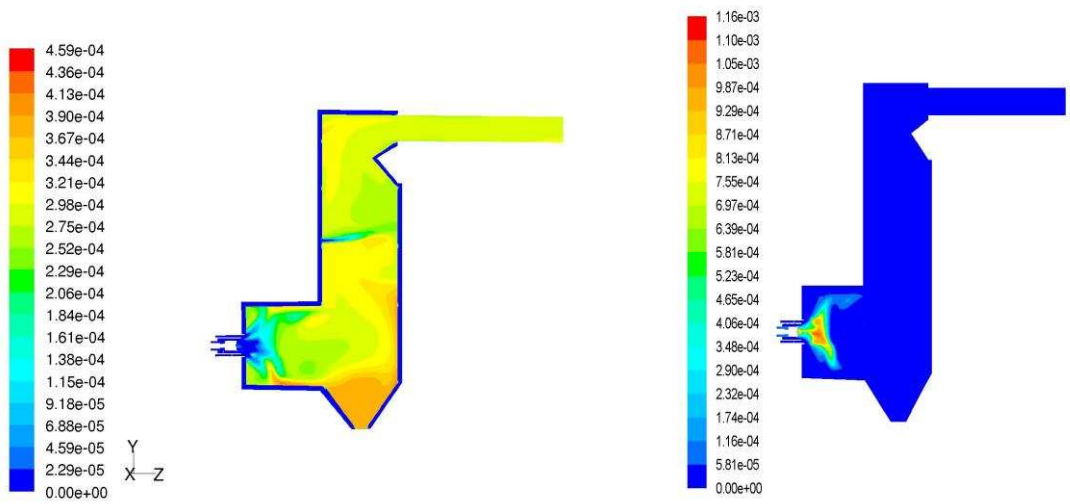


**Figure 4** (a) Computed NO<sub>x</sub> profile calculated using the NH<sub>3</sub> intermediate route only and using the De Soete equation. (b) NH<sub>3</sub> concentration profiles (mol fraction).

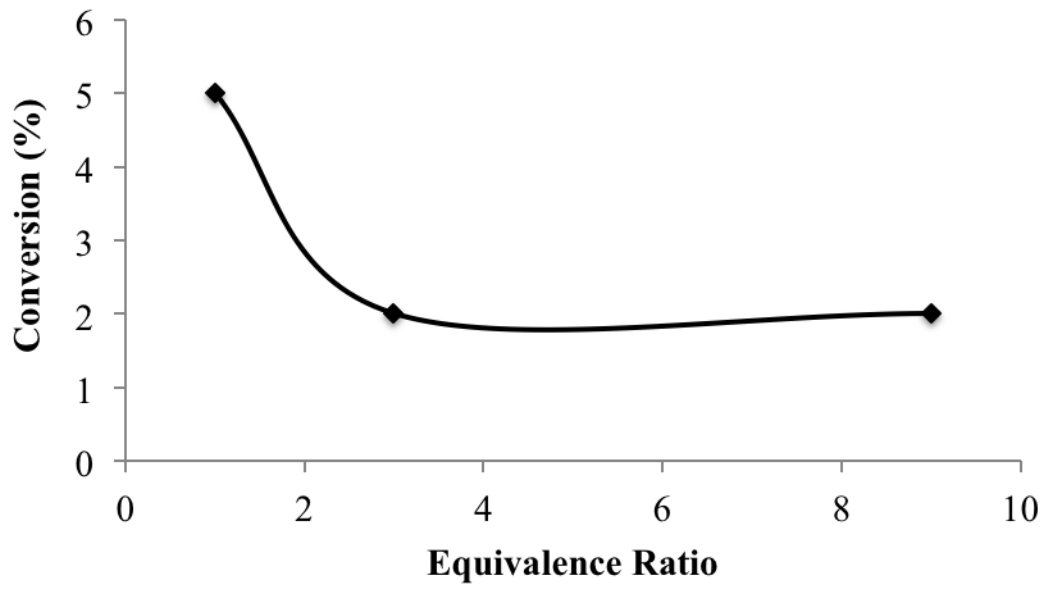


**Figure 5.** Percentage conversion to NO as a function of the equivalence ratio (based on (Chaiklangmuang et al., 2002)).

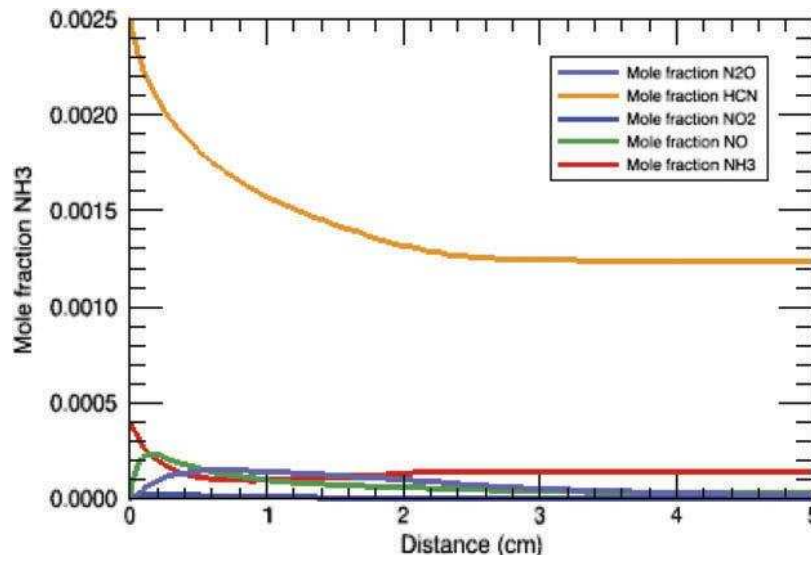


**Figure 6.** Plot of concentrations of NO, HCN, NH<sub>3</sub> in the primary zone as function of reactor distance (5 cm distance is equivalent to 0.1 s). Reactor temperature is 1000 K, equivalence ratio is 1.2.

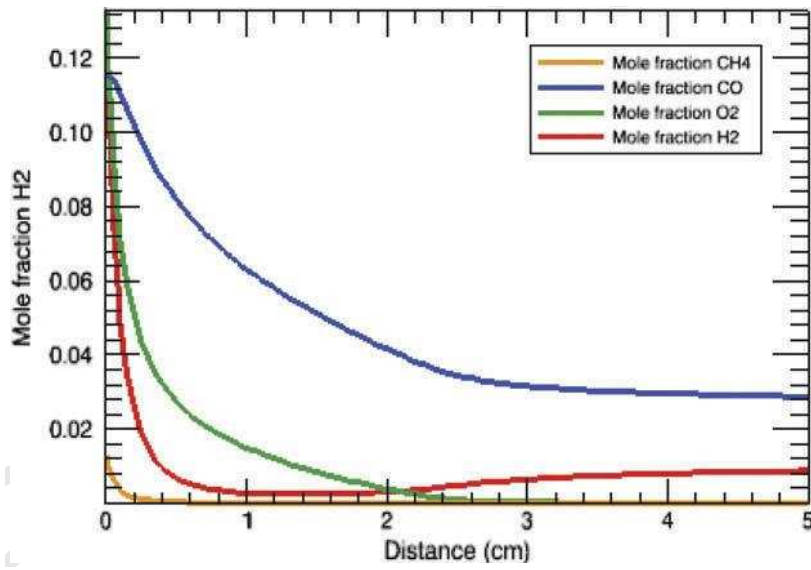


**Figure 7.** Plot of fuel components ( $\text{CH}_4$ ,  $\text{CO}$ ,  $\text{H}_2$ ) and  $\text{O}_2$  in the primary zone as a function of reactor distance. Same conditions as in Figure 6.

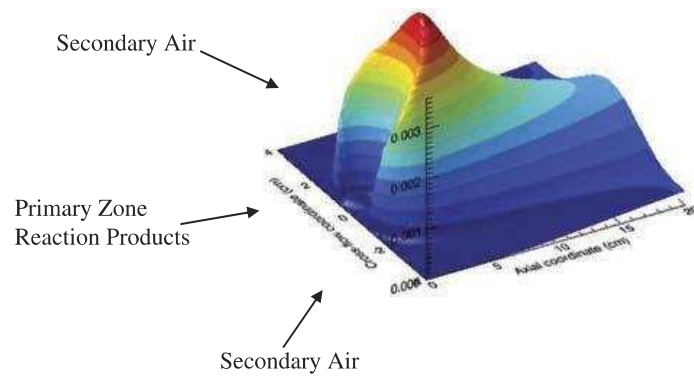


**Figure 8.** Computed results of the formation of additional NO in the secondary mixing zone. The primary zone products enter from the bottom left-hand corner.